Electronic Supplementary Material (ESI) for RSC Advances.

Supporting information

A novel tetraethylenepentamine functionalized polymeric adsorbent for enhanced removal and selective recovery of heavy metal ions from saline solutions

Xiao-Peng Zhang,[ab] Fu-Qiang Liu,[a] Chang-Qing Zhu,[a] Chao Xu,[a] Da Chen,[a] Meng-Meng Wei,[a] Jian Liu,[b] Cheng-Hui Li,[b] Chen Ling,[a] Ai-Min Li[a] and Xiao-Zeng You[b]*

[a]State Key Laboratory of Pollution Control and Resource Reuse, School of the Environment, Nanjing University, Nanjing 210046, People's Republic of China, E-mail: jogia@163.com; Fax: +86-25-89680377; Tel: +86-25-89680377

[b]State Key laboratory of Coordination Chemistry, School of Chemistry and Chemical Engineering, Collaborative Innovation Center of Advanced Microstructures, Nanjing university, Nanjing 210093, People's Republic of China

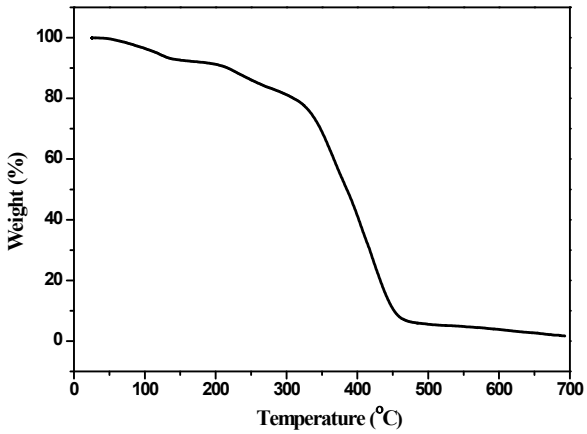

Fig. S1 TGA curve of PAMD.

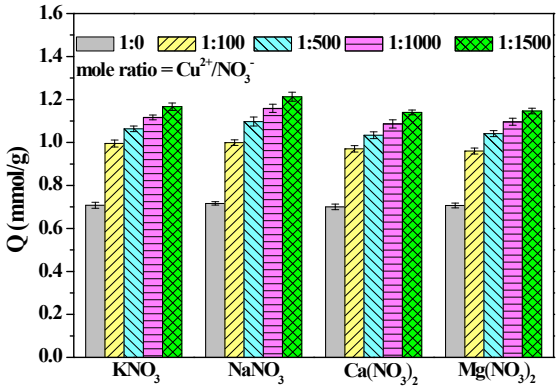

Fig. S2 Adsorption performances of Cu(II) onto PAMD in different nitrate systems.

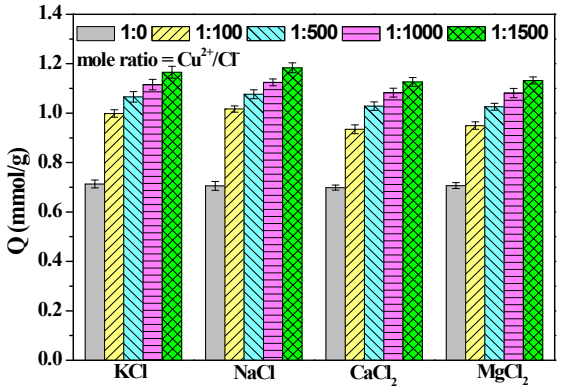

Fig. S3 Adsorption amounts of Cu(II) onto PAMD with different concentrations of a series of chlorides.

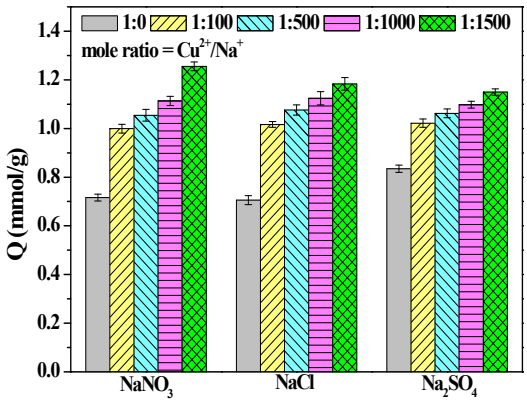

Fig. S4 Adsorption amounts of Cu(II) onto PAMD with different concentrations of a series of sodium salts.

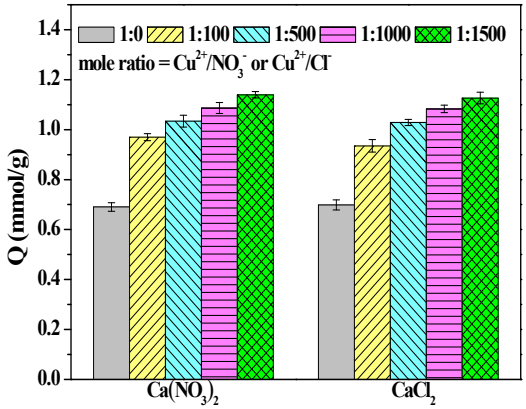

Fig. S5 Adsorption amounts of Cu(II) onto PAMD with different concentrations of a series of calcium salts.

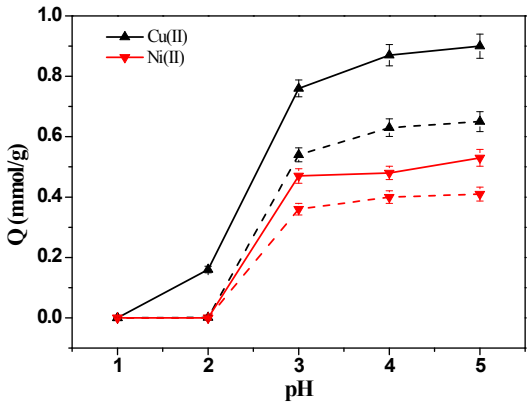

Fig. S6 Effect of pH on the sorption of Cu(II) and Ni(II) onto PAMD (solid line) and S984 (dash line) in sole system.

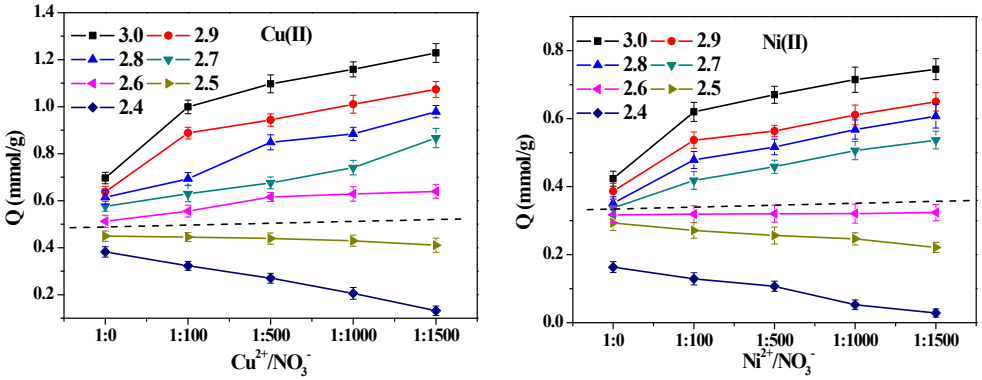

Fig. S7 Adsorption amounts of Cu(II) (left) and Ni(II) (right) as a function of aqueous pH-value in Cu(II)/ $NaNO_3$ or Ni(II)/$NaNO_3$ binary systems.

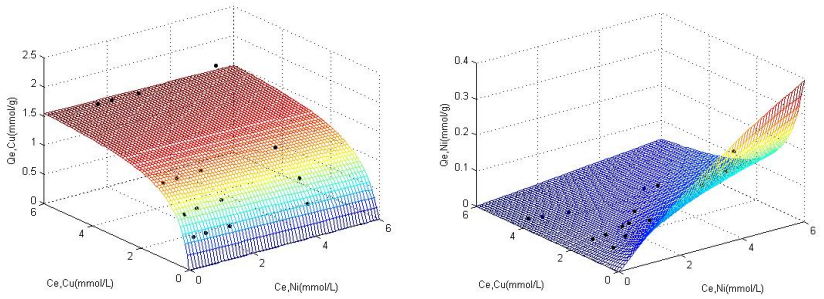

(a)

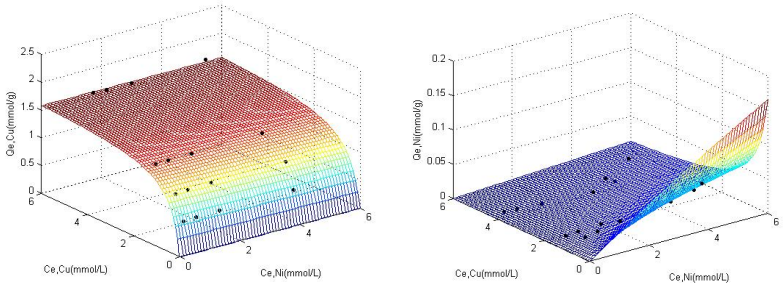

(b)

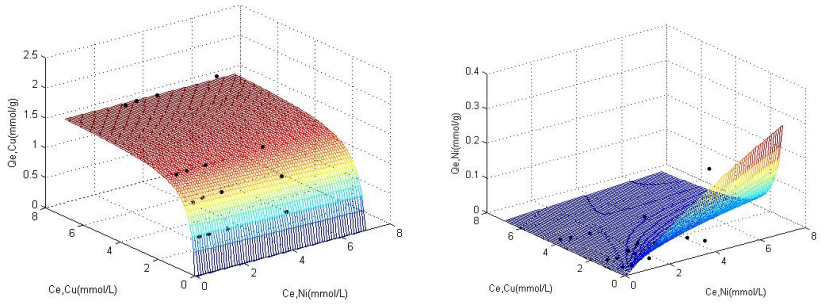

(c)

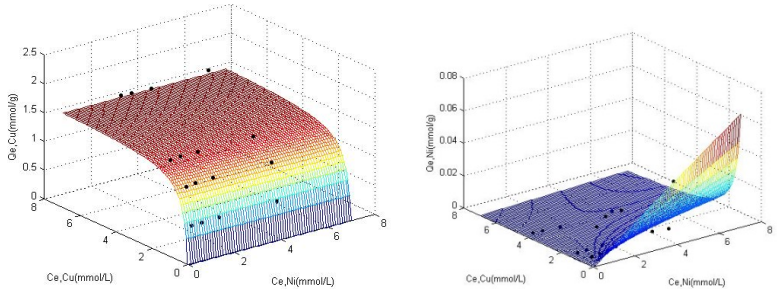

(d)

Fig. S8 Three-dimensional isotherm surfaces of PAMD simulated with the modified Langmuir model from: (a) Cu(II)/Ni(II) binary systems, (b) Cu(II)/Ni(II)/$NaNO_3$ (10 mmol/L) ternary systems, (c) Cu(II)/Ni(II)/$NaNO_3$ (100 mmol/L) ternary systems, (d) Cu(II)/Ni(II)/$NaNO_3$ (1500 mmol/L) ternary systems**.**

Table S1 Parameters of Cu(II)/Ni(II) binary and Cu(II)/Ni(II)/$NaNO_3$ ternary isotherm models for the adsorption of Cu(II) and Ni(II) onto PAMD.

Cu(II)/Ni(II)/$NaNO_3$	Modified Langmuir	Extended Langmuir
0 mmol/L	RSS=1.3602	RSS=0.1283
parameters	η_{Cu}=2.1843	Qmax=2.7839
	η_{Ni}=15.4302	K_{Cu}=0.4680; K_{Ni}=0.0201
10 mmol/L	RSS=1.4261	RSS=0.0829
parameters	η_{Cu}=1.7244	Qmax=2.8441
	η_{Ni}=21.4421	K_{Cu}=0.6727; K_{Ni}=0.0178
100 mmol/L	RSS=2.1138	RSS=0.1527
parameters	η_{Cu}=1.2013	Qmax=2.8876
	η_{Ni}=25.0151	K_{Cu}=0.8258; K_{Ni}=0.0116
1500 mmol/L	RSS=2.4425	RSS=0.1511
parameters	η_{Cu}=1.0348	Qmax=2.9011
	η_{Ni}=131.5789	K_{Cu}=0.9748; K_{Ni}=0.0024

Table S2 Separation factors α_{Ni}^{Cu} in binary and ternary systems for PAMD.

C_{NaNO3}	Ni(II) / Cu(II)	0.5 mmol/L	1.0 mmol/L	2.0 mmol/L	5.0 mmol/L
0 mmol/L	0.5 mmol/L	4.46	7.10	10.25	23.67
	1.0 mmol/L	8.42	14.64	20.63	27.82
	2.0 mmol/L	10.94	16.00	23.15	29.79
	5.0 mmol/L	29.35	74.08	560.53	1160.19
	Ni(II) / Cu(II)	0.5 mmol/L	1.0 mmol/L	2.0 mmol/L	5.0 mmol/L
10 mmol/L	0.5 mmol/L	6.38	11.59	19.76	104.88
	1.0 mmol/L	27.49	45.79	72.71	122.40
	2.0 mmol/L	37.26	70.33	105.55	201.15
	5.0 mmol/L	149.34	236.03	787.93	1984.33
	Ni(II) / Cu(II)	0.5 mmol/L	1.0 mmol/L	2.0 mmol/L	5.0 mmol/L
100 mmol/L	0.5 mmol/L	12.23	19.28	47.09	129.71
	1.0 mmol/L	29.48	238.27	296.28	455.36
	2.0 mmol/L	75.21	285.51	448.67	576.80
	5.0 mmol/L	159.79	640.84	1283.12	4803.94
	Ni(II) / Cu(II)	0.5 mmol/L	1.0 mmol/L	2.0 mmol/L	5.0 mmol/L
1500 mmol/L	0.5 mmol/L	33.47	55.57	104.84	202.48
	1.0 mmol/L	388.17	672.83	731.62	1180.71
	2.0 mmol/L	502.36	845.25	1232.02	2454.26
	5.0 mmol/L	667.34	1315.64	2630.07	→∞

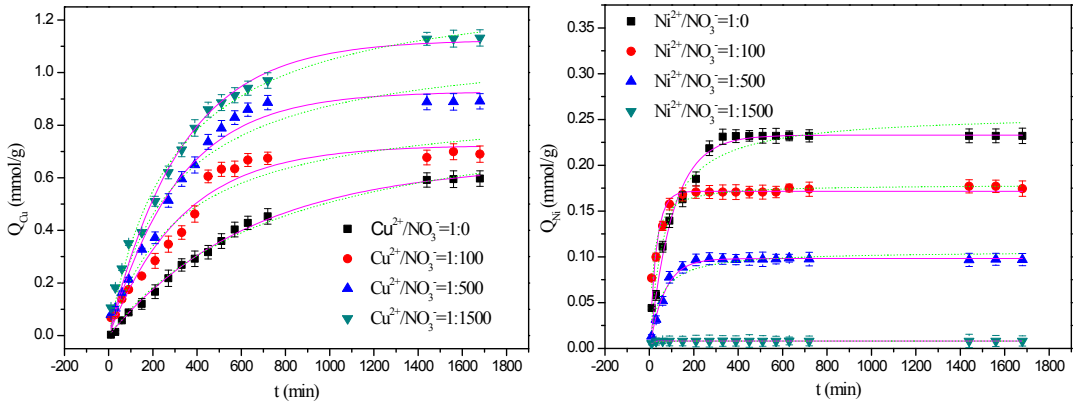

Fig. S9 Kinetic adsorption behaviors of Cu(II) and Ni(II) in Cu(II)/Ni(II) binary and Cu(II)/Ni(II)/$NaNO_3$ ternary systems.

Table S3 Kinetic rate parameters for the adsorption of Cu(II) and Ni(II) in Cu(II)/Ni(II) binary and Cu(II)/Ni(II)/$NaNO_3$ ternary systems.

Concentration of $NaNO_3$（mmol/L）	Metals	First-order			Second-order			
		qe	k_1	r^2	qe	k_2	r^2	h
0	Cu(II)	0.65651	0.00156	0.99658	0.91294	0.00136	0.9931	0.001133
	Ni(II)	0.23291	0.00955	0.98035	0.25719	0.05395	0.96363	0.003569
100	Cu(II)	0.72408	0.003	0.96518	0.88856	0.00351	0.93697	0.002771
	Ni(II)	0.17159	0.03231	0.90368	0.32915	0.17894	0.9586	*
500	Cu(II)	0.92804	0.00322	0.98194	1.12786	0.00305	0.9571	0.00388
	Ni(II)	0.09815	0.01464	0.9909	0.1063	0.20381	0.94174	*
1500	Cu(II)	1.12438	0.00308	0.98494	1.35483	0.00253	0.98831	0.004644
	Ni(II)	0.00814	0.10434	0.98886	0.0082	33.04505	0.82099	*

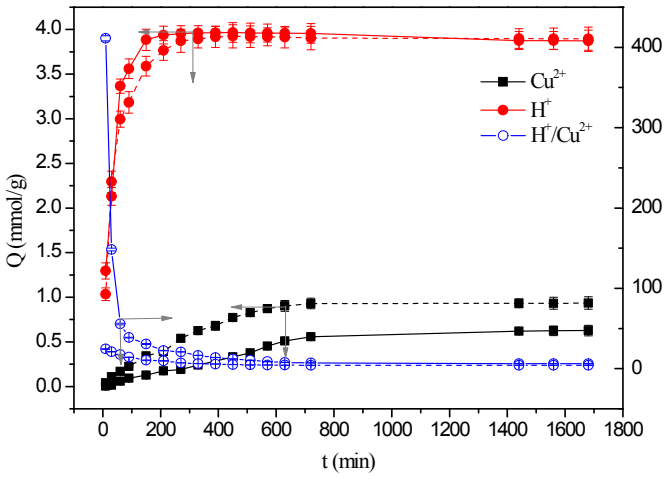

Fig. S10 Time course of adsorbed H^+, Cu^{2+} and H^+/Cu^{2+} in Cu(II)/Ni(II) (solid line) binary system and Cu(II)/Ni(II)/$NaNO_3$ (500 mmol/L) (dash line) ternary system.

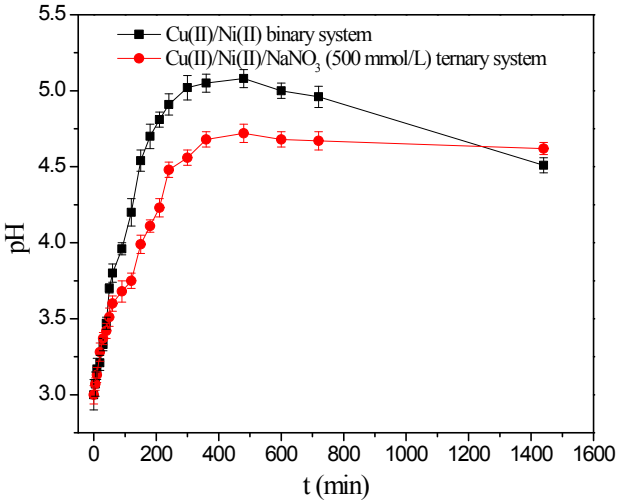

Fig. S11 Time course of pH in Cu(II)/Ni(II) binary system and Cu(II)/Ni(II)/$NaNO_3$ (500 mmol/L) ternary system.

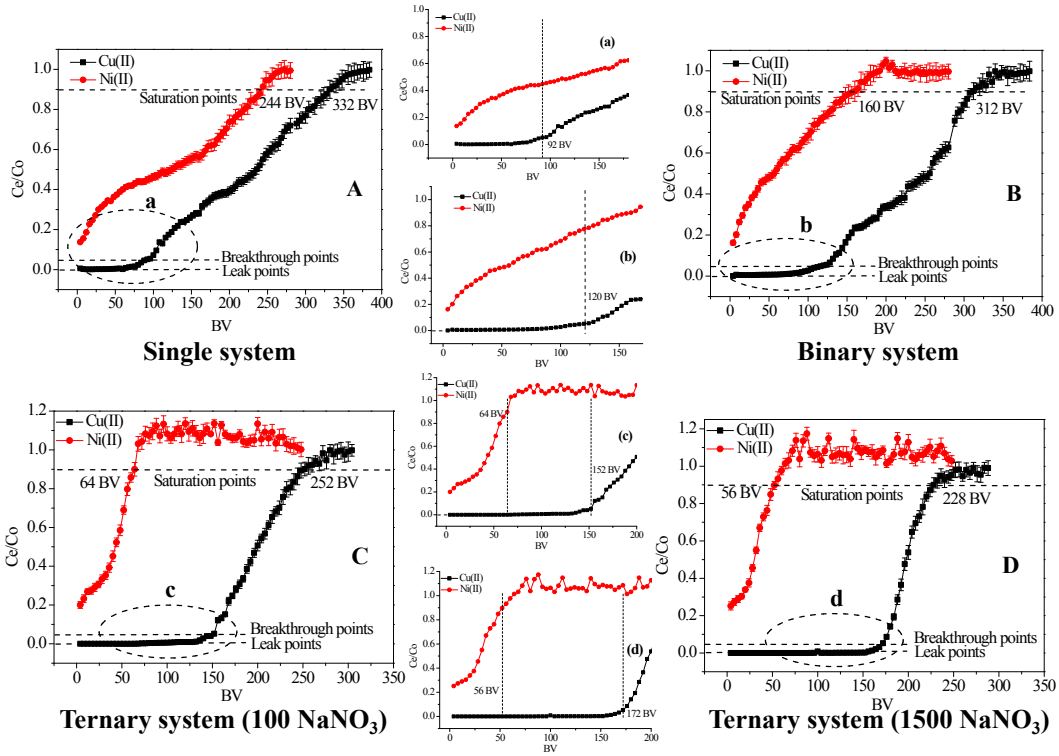

Fig. S12 Breakthrough curves for Cu(II) and Ni(II) from different dynamic adsorption systems.

Table S4 Breakthrough curves parameters for adsorptions of Cu(II) and Ni(II) onto PAMD in different dynamic systems.

PAMD	Heavy metal ions	Breakthrough pints (BV)	Saturation points (BV)
Single system	Cu(II)	92	332
	Ni(II)	4	244
Binary system	Cu(II)	120	312
	Ni(II)	1	160
Ternary system (100 mmol/L $NaNO_3$)	Cu(II)	152	252
	Ni(II)	0.5	64
Ternary system (1500 mmol/L $NaNO_3$)	Cu(II)	172	228
	Ni(II)	0.5	56

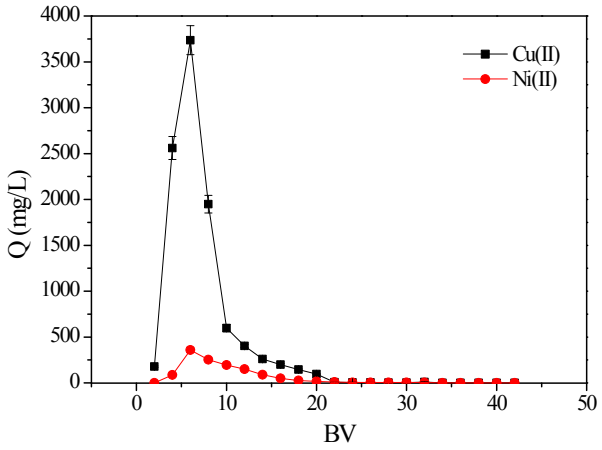

Fig. S13 Desorptions of PAMD for Cu(II) and Ni(II) in single system.

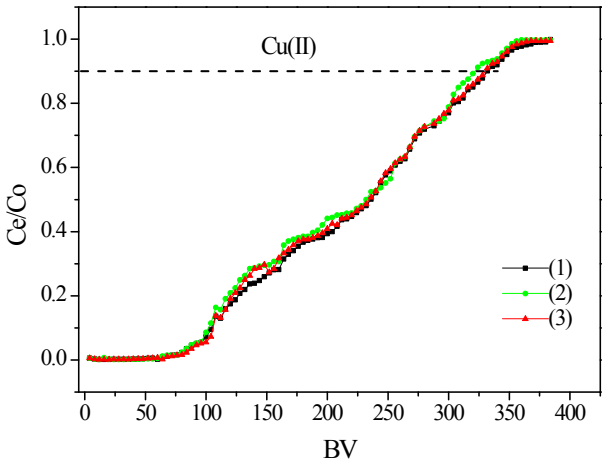

Fig. S14 Regeneration and reuse of PAMD with 15% HCl.

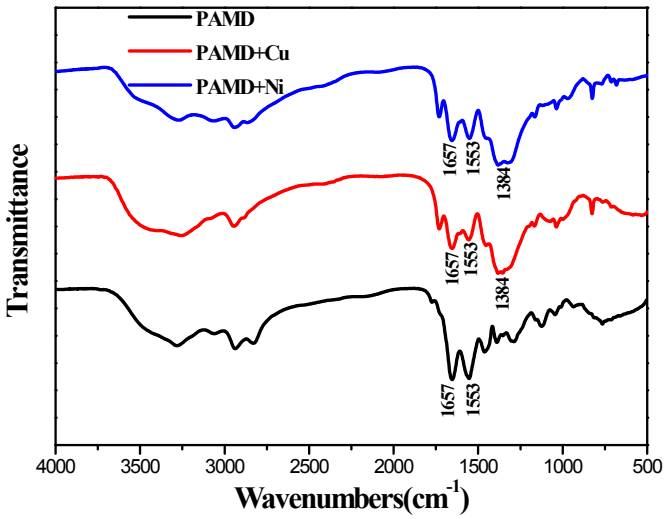

Fig. S15 FTIR spectra of PAMD before and after adsorption.

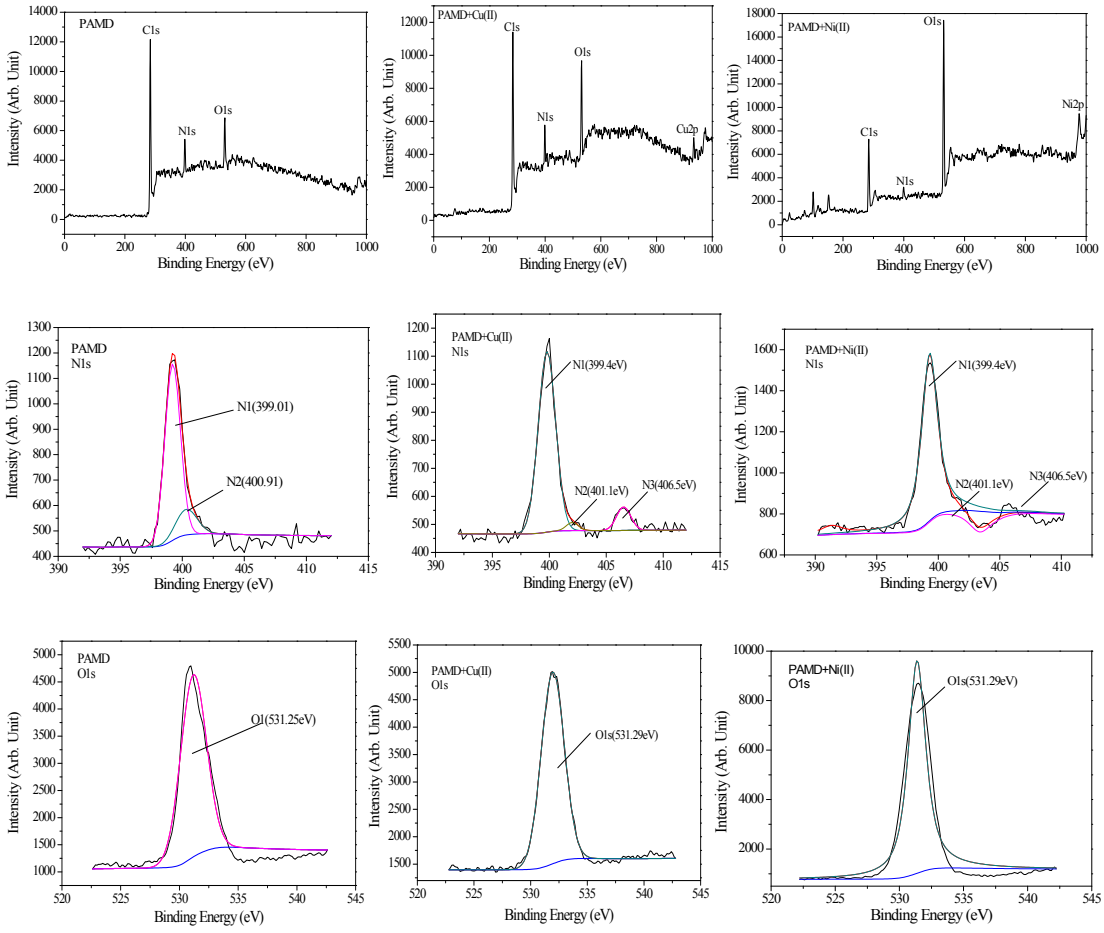

Fig. S16 XPS spectra of PAMD before and after adsorbing Cu(II) and Ni(II).

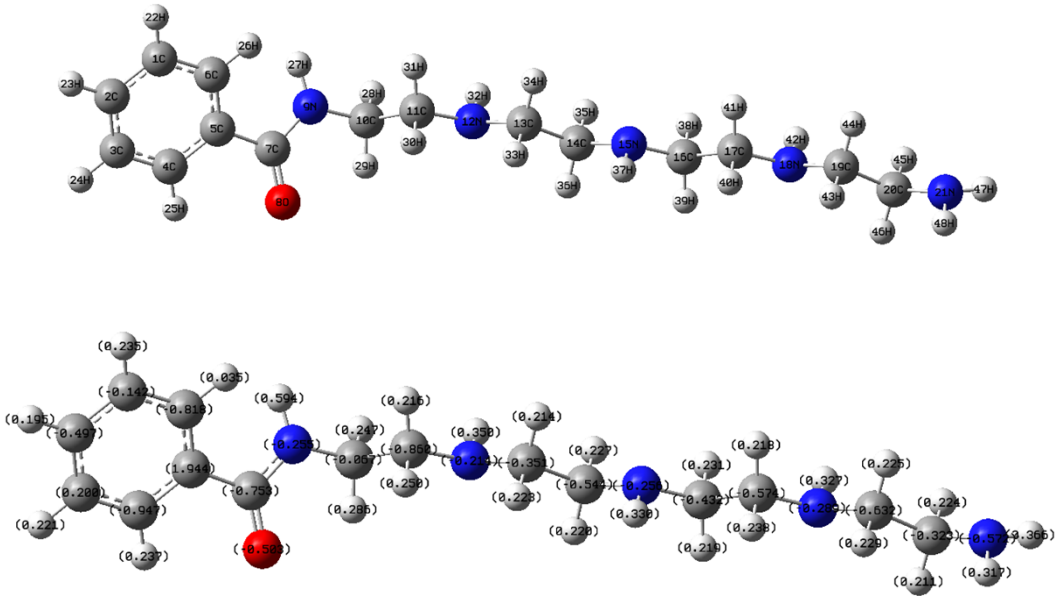

Fig. S17 The Mulliken atomic charge distribution of PAMD.

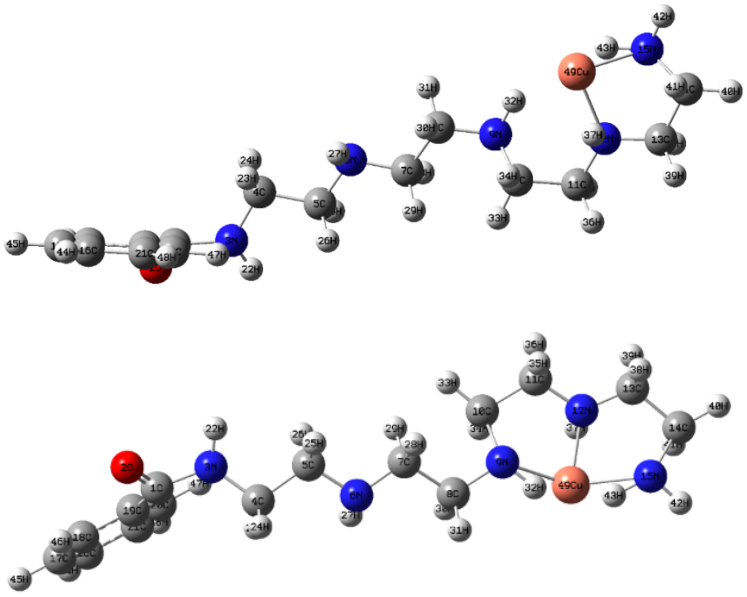

Fig. S18 Coordination modes for Cu(II) ions on PAMD (upper: Complex-I; bottom: Complex-II).

Table S5 Selected optimized geometrical parameters of complexes.

	PAMD	Complex-I	Complex-II
ΔE(kJ/mol)		-2344.65	-1987.36

Bond length(Å)	C14-N15	1.469	C8-N9	1.457	C8-N9	1.457	C8-N9	1.457
	N15-C16	1.470	N9-C10	1.456	N9-C10	1.631	N9-C10	1.631
	C17-N18	1.469	C11-N12	1.456	C11-N12	1.455	C11-N12	1.455
	N18-C19	1.469	N12-C13	1.455	N12-C13	1.455	N12-C13	1.455
	C20-N21	1.467	C14-N15	1.454	C14-N15	1.500	C14-N15	1.500
			N12-Cu49	1.95	N19-Cu49	1.96	N19-Cu49	1.96
			N15-Cu49	1.95	N12-Cu49	1.96	N12-Cu49	1.96
					N15-Cu49	2.06	N15-Cu49	2.06
Bond angle(°)	C14-N15-C16	115.9	C8-N9-C10	115.07	C8-N9-C10	99.02	C8-N9-C10	99.02
	N15-C16-C17	110.7	N9-C10-C11	110.1	N9-C10-C11	92.37	N9-C10-C11	92.37
	C17-N18-C19	116.8	C11-N12-C13	114.2	C11-N12-C13	114.2	C11-N12-C13	114.2
	N18-C19-C20	110.9	N12-C13-C14	110.0	N12-C13-C14	110.0	N12-C13-C14	110.0
	C19-C20-N21	110.7	C13-C14-N15	110.3	C13-C14-N15	110.7	C13-C14-N15	110.7
			C13-N12-Cu49	97.8	C8-N9-Cu4	127.73	C8-N9-Cu4	127.73
			C14-N15-Cu49	102.7	C10-N9-Cu49	116.27	C10-N9-Cu49	116.27
			N12-Cu49-N15	94.0	N9-Cu49-N12	81.98	N9-Cu49-N12	81.98
					C13-N12-Cu49	107.1	C13-N12-Cu49	107.1
					C14-N15-Cu49	107.0	C14-N15-Cu49	107.0
					N12-Cu49-N15	87.1	N12-Cu49-N15	87.1

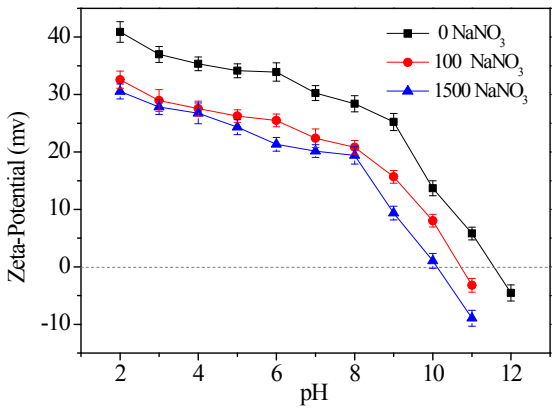

Fig. S19 -potential of PAMD at different solution pH values and salt concentrations.

Table S6 Characteristic parameters of Cu(II) and Ni(II).

Metal ions	$\|log K_{MOH}\|$	δ	*IP*	Z^2/r
Cu(II)	6.00	0.104	7.73	283.03
Ni(II)	4.14	0.126	18.17	237.13

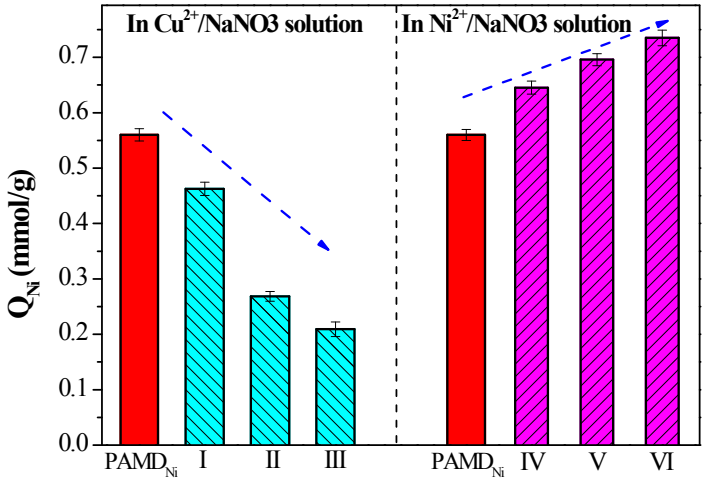

Fig. S20 Preloading experiments at pH = 3: the PAMD beads adsorbed with nickel at 0.56 mmol/g ($PAMD_{Ni}$). Then these beads were placed in the different systems. I: in $Cu(NO)_3$ solution; II: in Cu^{2+}+$NaNO_3$ (100 mmol/L) solution; III: in Cu^{2+}+$NaNO_3$ (200 mmol/L) solution; IV: in $NaNO_3$ (1 mmol/L) solution; V: in $NaNO_3$ (100 mmol/L) solution; VI: in $NaNO_3$ (200 mmol/L) solution.

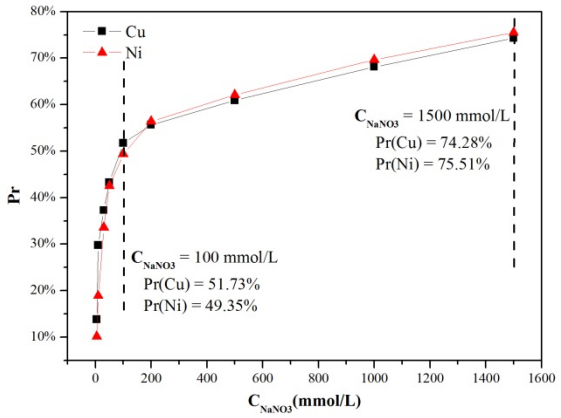

Fig. S21 Promotion ratios (Pr) of Cu(II) and Ni(II) in Cu(II)/Na(I) and Ni(II)/Na(I) binary systems with different concentrations of $NaNO_3$.

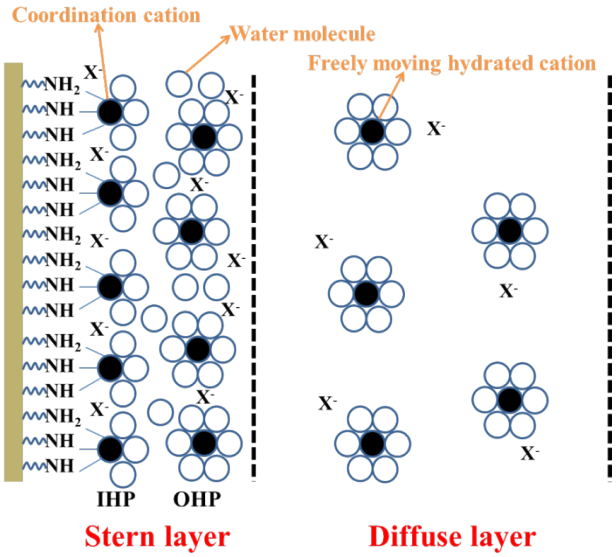

Fig. S22 Schematic picture of EDL in the adsorption system regarding polyamine resins.